Heat exchanges in the heterothermic zone of a karst system: Monlesi cave, Swiss Jura Mountains

Marc Luetscher, Baudouin Lismonde, Pierre-Yves Jeannin

Heat exchanges in the heterothermic zone of a karst system: Monlesi cave, Swiss Jura Mountains

Marc Luetscher,[1,2] Baudouin Lismonde,[3] and Pierre-Yves Jeannin[4]

Subsurface ice accumulations in temperate karst environments are assumed to be highly sensitive to external climate forcing and therefore represent a favorable setting for studying processes controlling heat exchanges in the heterothermic zone of a karst system. Air, rock, water, and ice temperatures were measured and complemented by airflow, water discharge, and cave air humidity data during a case study carried out between 2001 and 2006 at Monlesi ice cave in the Swiss Jura Mountains. The energy balance of the system could be quantified for an annual cycle, and results demonstrate that forced convection, which is controlled by the temperature difference between the cave air and the external atmosphere, is a driving force for the heat exchange between the cave and the surrounding environment. Therefore compared to the external mean annual conditions, major thermal anomalies are to be expected in the entrance zone of a cave system. Since this heterothermic zone may extend over several hundreds of meters, a better understanding of the mechanisms controlling the subsurface deposition environment represents a major prerequisite for high-resolution paleoenvironmental reconstructions from cave deposits.

1. Introduction

[2] Paleoenvironmental reconstructions from cave deposits are largely based on the assumption of a stable subsurface climate system, characterized by attenuated daily and annual air temperature fluctuations, high relative humidity, and minor changes in the cave pCO_2, which together favor calcite precipitation close to equilibrium with the cave's atmosphere [*Hendy*, 1971]. However, several authors have underlined the difficulty of interpreting and comparing speleothem data because of the site-specific factors that may influence the record [e.g., *McDermott*, 2004; *Fairchild et al.*, 2006, and references therein]. Indeed, recent articles reported seasonal air temperature oscillations of several degrees from ventilated cave systems [e.g., *Johnson et al.*, 2006; *Lacelle et al.*, 2004; *Roberts et al.*, 1998], suggesting that modifications of the cave microclimate and hydrology from the model ideal must have occurred. In order to assess the impact of changing climatic conditions on cave environments, a better understanding of subsurface heat and mass transfers is necessary.

[3] The temperature distribution in mature karst systems is largely controlled by advective fluxes from water and air circulations [*Luetscher and Jeannin*, 2004a]. For "fossil" cave passages, which have been abandoned by their formative streams, fluxes due to air circulation are typically the most important. Several mechanisms drive subsurface air circulation, including density-driven flows, barometric fluctuations, and diphasic flow due to water circulation. Of these, forced convection induced by internal-external temperature contrasts in multiple cave entrances is probably the most significant [e.g., *Andrieux*, 1969; *Wigley and Brown*, 1976; *Badino*, 1995; *Lismonde*, 2002, and references therein]. During the winter season, when cave air is warmer and less dense than the external atmosphere, it discharges from upper entrances, and colder external air is drawn in from lower entrances. As this air flows through the cave, it undergoes changes in temperature and relative humidity as a result of the heat transferred to and from the cave walls. The ventilation is maintained until the pressure difference between the cave and the external atmosphere is insufficient to force circulation. Because of seasonal and diurnal air temperature oscillations in the external atmosphere, cave airflow direction can be reversed. Thus lower entrances experience a strong winter cooling, and upper entrances experience a strong summer warming, resulting in systematic contrast between these sites and regional average temperature. This "heterothermic zone" sometimes extends up to several hundreds of meters into the cave and is subject to seasonal temperature oscillations. *Wigley and Brown* [1971] characterized the decrease of air temperature with distance into a conduit with unidirectional air circulation by a relaxation length which is function of the distance from the cave entrance to obtain thermal equilibrium. Empirical

[1]School of Geographical Sciences, University of Bristol, Bristol, UK.
[2]Now at Institute of Geology and Paleontology, University of Innsbruck, Innsbruck, Austria.
[3]Laboratory of Geophysical and Industrial Fluid Flows, Domaine Universitaire, Grenoble, France.
[4]Swiss Institute for Speleology and Karstology, La Chaux-de-Fonds, Switzerland.

calibration of their model with data from Glowworm cave, New Zealand, enabled *de Freitas et al.* [1982] and *de Freitas and Littlejohn* [1987] to determine the spatial and temporal distribution of cave air temperature as a function of the external atmospheric conditions. Seasonal air temperature oscillations of at least 4.5°C were measured in the most remote parts of Glowworm cave, suggesting that the entire cave belongs to the heterothermic zone. More recently, it was demonstrated that cave ventilation patterns also affect the subsurface atmospheric composition, condensation rates [e.g., *de Freitas and Schmekal*, 2003], CO_2 concentrations [*Baldini et al.*, 2006; *Bourges et al.*, 2001, 2006; *Spötl et al.*, 2005], and radon levels [*Atkinson et al.*, 1983; *Dueñas et al.*, 1999].

[4] In temperate karst environments, explanation of the survival of subsurface ice accumulations represents probably the most severe test for models of the magnitude and direction of heat and mass transfers induced by cave air circulation. In particular, some perennial ice accumulations are preserved in caves where the external mean annual air temperature is several degrees above 0°C, and these represent interesting ''end-members'' in the processes controlling subsurface climate dynamics. Although cave ice deposits in temperate alpine caves have been widely reported in the past [e.g., *Balch*, 1970], relatively few authors have investigated heat transfers in such cave systems [e.g., *Bock*, 1913; *Saar*, 1956], and little is known about the processes controlling the mass balance of perennial subsurface ice deposits and its evolution under changing climate conditions [e.g., *Piasecki et al.*, 2006, and references therein]. Our study attempts to document the energy and mass fluxes of Monlesi ice cave in the Swiss Jura Mountains and to compile these measurements into an energy balance model. This ''easily'' accessible study site therefore offers a favorable environment for the general investigation of heat exchanges in the heterothermic zone of a karst system and for assessing their response to changing climatic conditions.

2. Study Site

[5] Monlesi ice cave, located in the Swiss Jura Mountains (6°35′4″E, 46°56′18″N, 1135 m above sea level (asl) (Figure 1)), opens on the floor of a large closed depression which forms one of several aligned along the axis of a regional syncline. The host rock is characterized by massive, decimetric-layered micritic limestone which is locally densely fractured. The external mean annual air temperature (MAAT) measured outside the cave between 2001 and 2006 is 4.3 ± 0.4°C with a maximum annual range of nearly 50°C. Freezing conditions are experienced from November to April for about 2740 ± 318 h a^{-1}, which represents 30% of time of an annual cycle. The area has abundant precipitation (∼1500 mm a^{-1}), half of which falls in the form of snow over about 50 d a^{-1}. In presence of midwinter warm spells, the snow cover is, however, subject to partial melting in the course of the winter.

[6] The cave has three entrance shafts leading at −20 m to a large room 15 m high and 20 × 40 m in plan area. Because of the similar elevation of the shafts, the cave acts as a thermal trap, and air circulation is limited to a weak oscillating draft during the summer season. However, during the winter season, a strong unidirectional airflow is driven by the density difference between the external atmosphere and the cave air [*Luetscher and Jeannin*, 2004b]. This dense cold air enters the cave through the main shaft (diameter ø = 12 m), and the warmer air leaves the cave through the two smaller ones (ø = 6 and ø = 5 m, respectively), cooling the cave chamber and thus allowing the formation and preservation of a large perennial ice deposit. The ice forms a convex body with a maximum thickness of between 12 and 15 m and fills most of the cave chamber. The ice surface area is currently estimated at 900 m^2 (±10%), and the volume is approximately 6000 m^3, though uncertainties remain as to the exact geometry at the base of the deposit [*Luetscher et al.*, 2005]. The overall thickness of the stratified ice body is revealed in a 10 m face in the deepest part of the cave, the base of which is located 33 m below the ground surface.

[7] Although seasonal accumulation of snow is observed at the base of the entrance shafts, field observations suggest that the cave ice results mainly from cumulative freezing of percolation water entering via a limited number of drip points that form the locus for development during early winter and spring. The cave ice volume reaches its annual maximum in July, from which point ground heat, water percolation, and air circulation induce net ablation of the cave ice until the next cycle starts in December–January. While the formation of new cave ice commonly occurs at the top of the ice deposit, ablation may occur from all surfaces. In particular, heat exchanges at the ice-rock interface also result in the melting of the basal cave ice with an annual rate of 8 ± 2 cm a^{-1} [*Luetscher et al.*, 2007]. This rapid mass turnover rate was confirmed by multiproxy dating which provided an age of the lowest accessible ice layer of about 120 years old [*Luetscher et al.*, 2007].

3. Methods

3.1. Theoretical Approach

[8] A powerful method of quantifying external controls on heat exchanges within the cave system is to adopt a thermodynamic approach. The system under consideration comprises the three phases of water (including the cave ice, the seepage water, and snow inputs), the cave air, and the host rock mass. The system boundary conditions are defined by (1) a constant host rock temperature at a given distance from the cave walls and (2) exterior meteorological conditions at the entrances. Heat exchanges at the boundaries are characterized by (1) sensible and latent heat advection by airflow, (2) heat conduction through the limestone, (3) sensible and latent heat advection by water circulation and snow precipitation, and (4) solar radiation.

[9] The thermodynamic reference point is taken at the temperature of pure melting ice, and a zero enthalpy for dry air at 0°C was adopted. This supposes a zero enthalpy for water at 0°C, a positive enthalpy for water vapor, and a negative enthalpy for ice and snow (latent heat). Changes in the internal energy of the system during the year equal the sum of energies entering into the system less the sum of energies leaving the system. The annual energy balance of the system can thus be expressed from the following net flux and storage terms:

$$\Delta E_{\mathrm{air}} + E_{\mathrm{rock}} + \Delta E_{\mathrm{water}} + \mathrm{LE}_{\mathrm{snow}} + R = \Delta \mathrm{SE}_{\mathrm{ice}} + \Delta \mathrm{LE}_{\mathrm{ice}}, \quad (1)$$

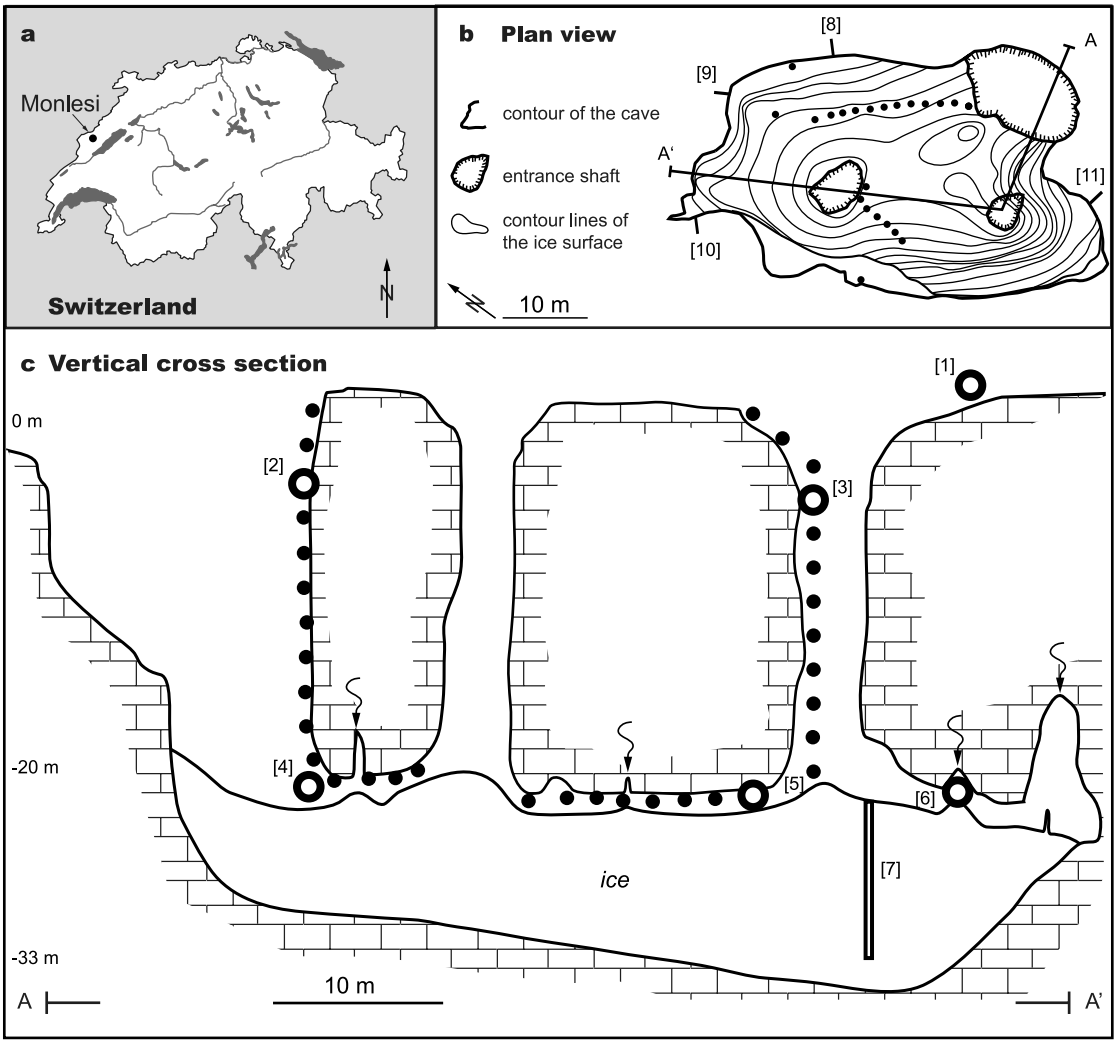

Figure 1. Plan view and cross section of Monlesi ice cave. Black dots locate the different thermistors, and main measurement stations are given by open circles, numbered (1) external temperature, precipitation, and barometric pressure; (2) temperature of in-flowing air; (3) temperature of out-flowing air; (4) air velocities and flow; (5) cave air temperature, air humidity, and ice extension; (6) water discharge and temperature; (7) cave ice temperature; (8) rock temperature from borehole 1; (9) rock temperature from borehole 2; (10) rock temperature from borehole 3; and (11) rock temperature from borehole 4.

where ΔE_{air} is sensible and latent heat advected by air circulation, E_{rock} is ground heat flux, ΔE_{water} is sensible heat advected by water circulation, LE_{snow} is latent heat of intrusive snow, R is solar radiation, ΔSE_{ice} is sensible heat stored in the cave ice, and ΔLE_{ice} is latent heat of ice.

[10] Here ΔLE_{ice} also represents the term related to the annual change of the cave ice mass; when $(\Delta SE_{ice} + \Delta LE_{ice}) > 0$, the mass balance of the cave ice is negative. To quantify the terms involved in the energy balance (1), sensible heat transfers at the boundaries of the system were assessed by the mean of temperature measurements carried out between 2001 and 2006. Latent heat exchanges were assessed on the basis of a number of assumptions validated by discontinuous field measurements of the cave air humidity and ice volume.

3.2. Field Measurements

[11] The cave environment presented several instrumentation challenges, including the cave atmosphere which has a humidity of nearly 100%, subzero freezing temperatures, and the abundance of seepage water. This led to several instrumental and power supply problems, such that full quantification of the energy balance was achieved only for the annual cycle in 2002–2003.

[12] Two main data acquisition stations were installed: one external to monitor surface conditions and one inside the cave. At the exterior station, a Campbell CR10X data logger with two multiplexer logging units was installed in a 745 × 535 × 300 mm polyester box. Power was supplied by a 20 W solar panel (BP Solar, type SX 20 U) with a Solsum 6.6 charge controller and a 12 V, 17 A h solar

accumulator. The accumulator was sufficient to provide 3 weeks of power in case of bad weather conditions. The data were transmitted weekly by GSM modem (9.6 kb) to a PC laptop. Inside the cave, a dataTaker DT 500 with a 10c multiplexer was powered by a 6 V, 12 A h battery, allowing about 3 months operation with the 30 min recording interval used. The data were recorded on a 2 Mb PCMCIA memory card which was sufficient for 3 months data storage.

[13] External air temperature was recorded 2 m above ground surface using a miniature temperature logger (UTL−1) shielded from direct solar radiation, and barometric pressure was measured using a Vaisala probe (PTB-100) connected to the external logging unit. Air temperature and barometric data recorded outside the cave agreed well (R^2 is 0.86 and 0.99, respectively) with those recorded at the Meteoswiss La Chaux-de-Fonds station (6°47′39″E, 47°04′32″N, 1060 m asl), located some 22 km northeast from the cave and at a comparable elevation. The latter station was therefore used as a complementary source for external meteorological data.

[14] Cave air temperatures were measured using negative temperature coefficient thermistors with a resistance of ∼29.5 kΩ at 0°C and a temperature coefficient of about 5% °C^{-1} (YSI 44006). The thermistors were sealed in silicon mass and heat-shrink tubing to protect them against external damages before being calibrated in a bath of melting ice to an accuracy of ±0.1°C. Thermistors were spaced at 2 m intervals in two chains, one down the main entrance shaft of the cave (23 thermistors) and one down the second shaft and along the cave roof (21 thermistors (Figure 1)). Air temperatures were recorded at 1 h intervals and logged externally.

[15] Airflow through the main cave entrance was derived from point velocity measurements sampled manually at different air temperatures using a Testo 425 digital thermo-anemometer. The point measurement was converted into flow using a rating curve derived from 22 spatially distributed measurement points over the 7.5 m^2 cross section. Final accuracy of airflow data is about ±10%.

[16] Cave air humidity was measured between 6 and 9 February 2004 using a mirror-type dew point hygrometer (Thygan VTP 37) placed within the airflow at the end of the cave room. The recording interval set by the manufacturer was 10 min, and accuracy is given as ±0.15°C or ±2% relative humidity (Hr). Power was supplied by a 12 V lead-acid accumulator. In absence of continuous power supply, it was technically impossible to monitor the cave air humidity for a longer time period.

[17] Precipitation at the site was measured using a 400 cm^2 0.2 mm resolution tipping bucket rain gauge 100 cm above ground level connected to the surface logging unit. The data are in good agreement with regional precipitation measured at two nearby pluviometric stations (MeteoSwiss) at similar elevations and distances of 5 and 13 km, respectively (La Brevine, 6°36′26″E, 46°58′48″N, 1042 m asl, and Les Ponts-de-Martel, 6°43′26″E, 47°0′18″N, 1060 m asl). The latter data were used in case of failure of our monitoring device on the basis of

$$P_{\text{Monlesi}} = 1.05*[(P_{\text{Brev}} + P_{\text{PDM}})/2], \quad (2)$$

where P_{Monlesi} is precipitation measured at Monlesi, P_{Brev} is precipitation measured at La Brevine, and P_{PDM} is precipitation measured at Ponts-de-Martel.

[18] The main water inlet (subcutaneous flow) was instrumented to measure discharge rates at a 30 min interval using a pressure probe set at the bottom of a 1 m long perforated PVC tube fed from the inlet. The measured water height (H, in m) was converted to discharge (Q, in L min^{-1}) with an empirically calibrated rating curve checked by manual gauging,

$$Q = 14.129*H - 3.988 \qquad 0.3 < H < 0.5 \quad (3)$$

$$Q = 30.724*H - 12.225 \qquad 0.5 > H > 1. \quad (4)$$

[19] Results are reliable for water discharge values ranging between 0.25 and 18.5 L min^{-1} with an accuracy estimated at ±10%. Because of technical problems, a gap in observations occurs in the active phase between 9 August and 25 September 2003. The missing data could, however, be reconstructed using an empirical recession curve based on three short-term events in July 2003 [*Luetscher*, 2005]. The advected heat provided by this water was assessed by simultaneously measuring water temperatures with a Pt-100 probe (±0.1°C) (Moser TMT, TR7c).

[20] Rock temperatures were measured in four 80 cm (40 mm diameter) long boreholes drilled in the cave walls equipped with Pt-100 probes (±0.1°C). The sensors were set at depths of −4, −22, −40, −58, and −77 cm and isolated by polyurethane packers. To improve the heat conduction with the host rock, each probe was set previously into a copper ring of a diameter close in size to the borehole. Rock temperatures were recorded at 30 min time intervals using the subsurface data logger.

[21] Temperature of the 6000 m^3 layered congelation ice body was measured in an 8.5 m steam-drilled borehole centered on the top of the cave ice. After drilling on 28 February 2002, six Pt-100 sensors (±0.1°C) were positioned at depths of 0.1, 1, 2, 4, 5, and 8 m below the ice surface. Refreezing of the meltwater by the following day assured that the measurements were not contaminated. Ice temperature was recorded in 30 min time intervals with the cave data logger. Because of melting of the ice surface, the probe positioned at 0.1 m depth became exposed in October 2002 and was not used.

[22] Variation of the cave ice volume was determined manually by measuring the distance between the rock and the ice surface (±5 mm) at 11 reference stations located along the main airflow path. Although spatial variations of up to 40% were measured, one station, on the top of the ice body, was selected for a long-term monitoring of the cave ice extension. From 2004, the sporadic measurements from this station were complemented by an ultrasonic probe (Baumer Electric, UNAM 50) which was installed to monitor melting and accretion rates with a higher time resolution (12 h). The probe was calibrated against manual measurements, and final accuracy is of ±3 mm (n = 7); the data were used to extrapolate cave ice fluctuations between sporadic manual measurements. Assuming that measure-

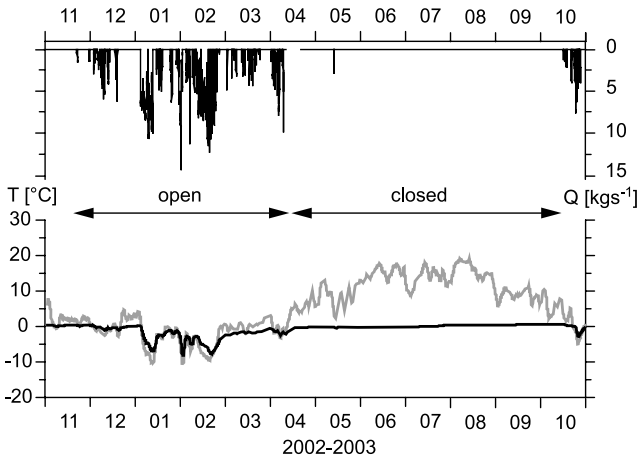

Figure 2. Air temperature and derived airflow recorded at Monlesi study site between November 2002 and October 2003. Recorded data highlight an open period from November to April which is characterized by a good correlation between the cave air temperature (black) and the surface temperature below freezing (gray).

ments are representative of the whole cave ice body, final precision on volume fluctuations is assessed at ±15%.

4. Results and Analysis

4.1. Cave Air Dynamics

[23] Figure 2 shows the air temperature measurements recorded at Monlesi ice cave between November 2002 and October 2003. During the summer period (roughly May to October), the cave exhibits a very stable temperature close to 0°C and is independent of surface temperature. Ventilation is reduced to a small oscillating airflow, suggesting the cave behaves as an aerodynamically closed "cold trap" system, with a stratified air column due to the higher density of cold air in the cave compared to warm external conditions. In absence of significant ventilation, the relative humidity reaches near saturation (Hr = 97.3 ± 0.6%).

[24] In contrast, between November and April, cave air temperatures follow closely those at the surface (R^2 = 0.80, n = 2263, significant at 1σ confidence interval), and the cave air humidity reaches values lower than 85%. The observed change in temperature inside the cave is associated with the surface air temperature falling below that of the cave, resulting in an unstable air column which allows ventilation to develop (open system conditions). Because convective heat exchanges with the external atmosphere increase with the diameter of the shaft, the cave experiences a unidirectional airflow from the base of the larger shaft toward the two smaller ones. However, since the flow paths show differentiated aeraulic resistances, most of the airflow (i.e., >80%) is directed toward the northern shaft. Although a buffering of air temperature is noted with distance into the cave, daily temperature oscillations measured by all thermistors suggest that thermal equilibrium is not reached inside the cave (Figure 3).

[25] The airflow derived from point velocity measurements varies between 1 and 15 $m^3\ s^{-1}$. For the maximum cave diameter of ~5 m, the equivalent Reynolds numbers range between 1.8×10^4 and 2.8×10^5, suggesting a fully developed turbulent airflow [e.g., *Incropera and DeWitt*, 2002]. A very good (R^2 = 0.99, n = 9) quadratic relation is therefore observed between the airflow and the temperature difference between the exterior and cave interior (Figure 4), which is consistent with the Darcy-Weisbach equation for fluid flow under turbulent conditions,

$$q_m = \sqrt{\frac{|\Delta P|}{R}}, \tag{5}$$

with ΔP defined by *Lismonde* [2002] as

$$\Delta P = \rho \frac{g}{273}(T_{\text{cave}} - T_{\text{ext}})H, \tag{6}$$

where q_m is airflow through the system (kg s^{-1}), ΔP is driving pressure (Pa), R is aeraulic resistance of the conduit ($kg^{-1}\ m^{-1}$), ρ is density of the cave air (kg m^{-3}), P_{cave} is barometric pressure inside the cave (Pa), P_{ext} is air pressure at the surface (Pa), T_{cave} is mean cave air temperature (K), T_{ext} is mean exterior temperature (K), and H is altitude difference between the entrances (m).

[26] During the 2002–2003 observation period, the system was subject to forced air convection for approximately 1150 h. The airflow was reconstructed for each time interval on the basis of the temperature measurements and the rating curve determined from equation (5). Results suggest that during the observation period, a total air volume of 13.6×10^6 m^3 transited through the cave (Figure 2). This supposes a mean airflow of ~3.3 $m^3\ s^{-1}$, which is consistent with the sporadic field measurements achieved manually during the open period between November and April.

4.2. Heat Advected by Air Circulation

[27] The convective heat exchange associated with subsurface air circulation can be determined from temperature and humidity measurements carried out at the extremities of the investigated system. Figure 5 shows the cave air temperature recorded at two of the entrance shafts during the 2003 open period (3–15 January 2003) together with the calculated airflow. Neglecting the temporal derivative of the internal energy of the air, incoming energy fluxes equal the outgoing fluxes. The heat removed from the system is therefore given by

$$\Delta E_{\text{air}} = \int_{\text{time}} Q_{\text{air}} \times \Delta h_s dt, \tag{7}$$

Figure 3. Temperature distribution in Monlesi ice cave measured during the summer (4 June 2003) and the winter season (1 February 2003). Because of the similar altitude of the cave entrances, a thermal stratification of the cave air is observed during the summer season. In contrast, a strong unidirectional air circulation is measured during the winter season, when the external air temperature is lower and thus denser than the cave air. Because of a lower aeraulic resistance, most of the airflow is drained toward one of the secondary shafts (gray arrows).

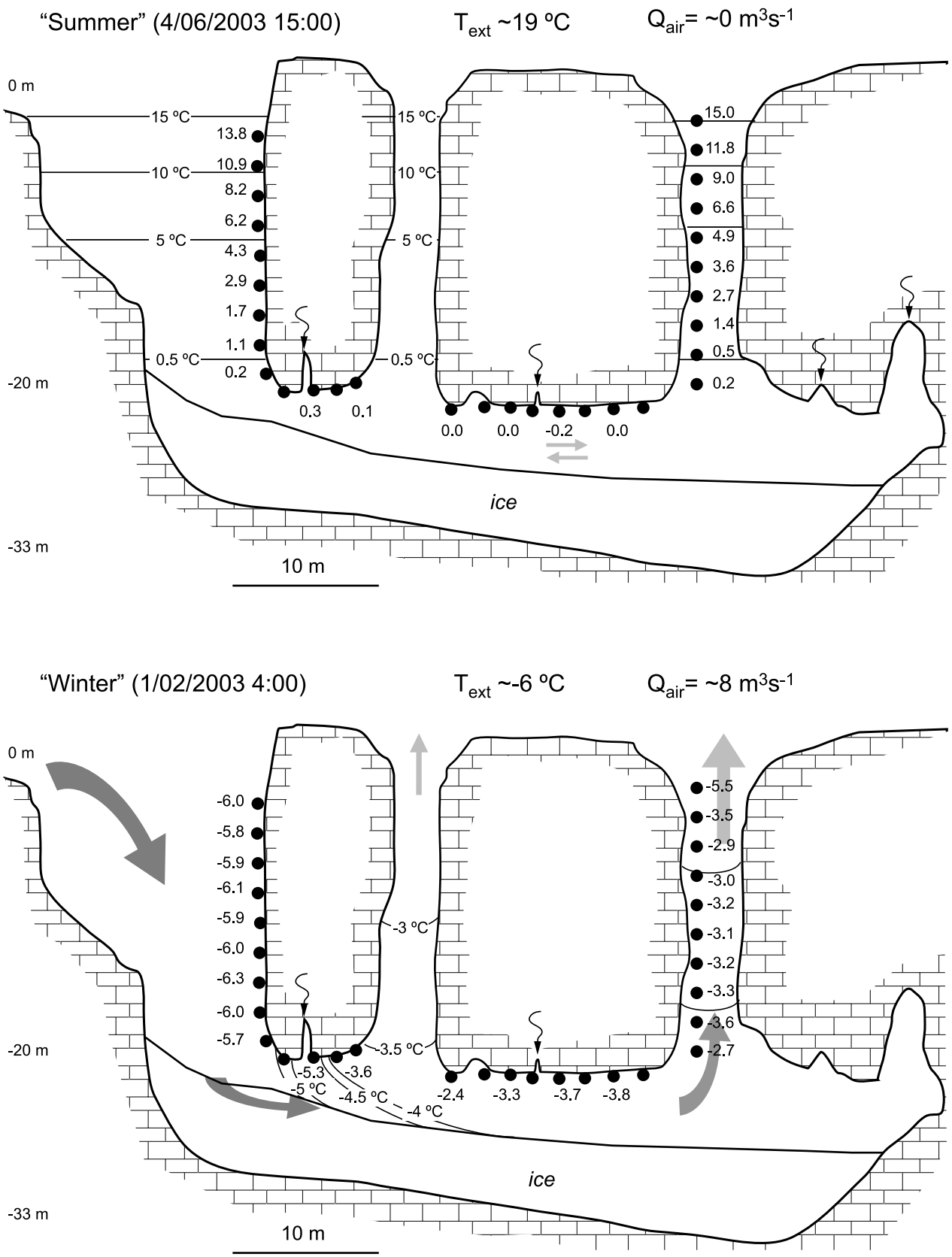
"Summer" (4/06/2003 15:00)
T_{ext} ~19 ºC
Q_{air}= ~0 m^3s^{-1}
0 m
15 ºC
10 ºC
5 ºC
0.5 ºC
13.8
10.9
8.2
6.2
4.3
2.9
1.7
1.1
0.2
0.3
0.1
15 ºC
10 ºC
5 ºC
0.5 ºC
15.0
11.8
9.0
6.6
4.9
3.6
2.7
1.4
0.5
0.2
0.0
0.0
-0.2
0.0
-20 m
ice
-33 m
10 m
"Winter" (1/02/2003 4:00)
T_{ext} ~-6 ºC
Q_{air}= ~8 m^3s^{-1}
0 m
-6.0
-5.8
-5.9
-6.1
-5.9
-6.0
-6.3
-6.0
-5.7
-3 ºC
-3.5 ºC
-5.3
-3.6
-5 ºC
-4.5 ºC
-4 ºC
-5.5
-3.5
-2.9
-3.0
-3.2
-3.1
-3.2
-3.3
-3.6
-2.7
-2.4
-3.3
-3.7
-3.8
-20 m
ice
-33 m
10 m

Figure 3

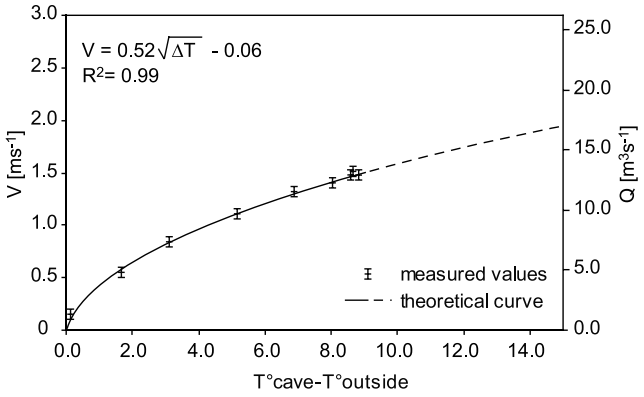

Figure 4. Air velocity and derived airflow measured for different temperature contrasts between the cave and the outside air.

where ΔE_{air} is energy removed from the system (J), Q_{air} is massic flow of dry air (kg s^{-1}), and Δh_s is difference in the specific enthalpy of humid air exchanged at the system boundaries (J kg^{-1}).

[28] Considering humid air as a mixture of ideal gases, the specific enthalpy h_s is given by

$$h_s = \frac{H}{m_{dry\_air}} = (c_{pa} + \omega c_{pv})T + \omega L_{vap}, \quad (8)$$

where

$$\omega = 0.622 \frac{p_v}{p - p_v}, \quad (9)$$

with H as enthalpy of air (J), m_{dry_air} as mass of dry air (kg), c_{pa} as heat capacity of dry air at constant pressure (J kg^{-1} K^{-1}), c_{pv} as heat capacity of vapor at constant pressure (J kg^{-1} K^{-1}), ω as specific humidity (kg $kg^{-1}_{dry\_air}$), T as temperature (K), L_{vap} as latent heat of vapor (2.5×10^6 J kg^{-1}), p_v as partial pressure of water (Pa), and p as air pressure (Pa).

[29] The airflow is derived from the air temperature measured with an hourly resolution, and the humidity of in-flowing air is derived from the humidity measured at the Chaux-de-Fonds meteorological station; it is also assumed that the out-flowing cave air is saturated. It becomes therefore possible to assess the energy advected by forced convection. During the 2002–2003 annual cycle, this energy exchange reached nearly -75 ± 8 GJ, more than 40% of it being attributed to latent heat exchanges due to evaporation/sublimation processes (i.e., 32 ± 3 GJ).

4.3. Conductive Heat Fluxes Through the Cave Walls

[30] Rock temperatures measured between November 2002 and October 2003 reveal seasonal oscillations through the entire length of the 80 cm deep drill holes, with attenuation of the signal and a phase shift increasing with depth (Figure 6). As the wall rock temperatures change from below freezing to above freezing between May and July, the rate of temperature changes, and in some cases (borehole 1) the thermal gradient, decreases. Abrupt temperature changes due to the thawing of pore water are also observed, in particular in borehole 2.

[31] However, an almost constant rock temperature gradient is observed during the summer season, when the cave air temperature is largely controlled by the melting of cave ice. Temperature gradients at that time range between 0.44 (borehole 4) and 0.7°C m^{-1} (borehole 2). Providing that on an annual average the temperature difference between the system boundaries and the cave walls remains constant, it is inferred that the measured gradient is representative of the annual heat conducted through the cave walls.

[32] For a homogeneous limestone having a heat conductivity of 2.2 W m^{-1} K^{-1}, this suggests a ground heat flux ranging between 1 and 1.5 W m^{-2} under steady state conditions, as given by Fourier's law (Table 1),

$$\varphi = -k \frac{dT}{dx}, \quad (10)$$

where φ is heat flux (W m^{-2}), k is thermal conductivity (W m^{-1} K), and dT/dx is the temperature gradient (K m^{-1}). The energy supplied by heat conduction through the cave walls is given by

$$E_{rock} = \int_{1year} \varphi S_{wall} dt, \quad (11)$$

where E_{rock} is energy issued from the ground heat flux (J), φ is density of heat flux (W m^{-2}), and S_{wall} is exchange surface area (m^2).

[33] Assuming that a constant heat flux of 1 ± 0.1 W m^{-2} is consistent with measurements from all but one of the boreholes. From the cave topographic survey, we derive an exchange surface of 4000 m^2 (±10%), corresponding to the rock-air and rock-ice interfaces. Therefore on the basis of equation (11), the energy diffused from the surrounding host rock can be assessed at 126 ± 25 GJ for the 2002–2003 observation period.

4.4. Heat Advected by Water Infiltration

[34] Discharge of seepage water into the cave was assessed during a high-water episode on 17 July 2002 after 36 h of continuous rain (56 mm 36 h^{-1}). Measured discharges vary from less than a few deciliters per minute to more than 15 L min^{-1}, with nearly half of the water entering the cave through a single inlet. Figure 7 illustrates the water discharge recorded at the main inlet of Monlesi ice cave between November 2002 and October 2003. Maximum measured flows reached nearly 15 L min^{-1} when the conduit was active. However, for 142 of the 365 d of the study period, the inlet was frozen, and discharge was zero.

[35] Analysis of 34 flood events at the main water inlet shows that discharge occurs with a time delay of 1 to 8 h

Figure 5. Air temperature and derived airflow recorded at the extremities of the ice cave system between 3 and 15 January 2003. Sensible heat exchanges account for nearly 60% of the total heat transfer. Latent heat exchanges were calculated assuming an out-flowing air saturated in humidity.

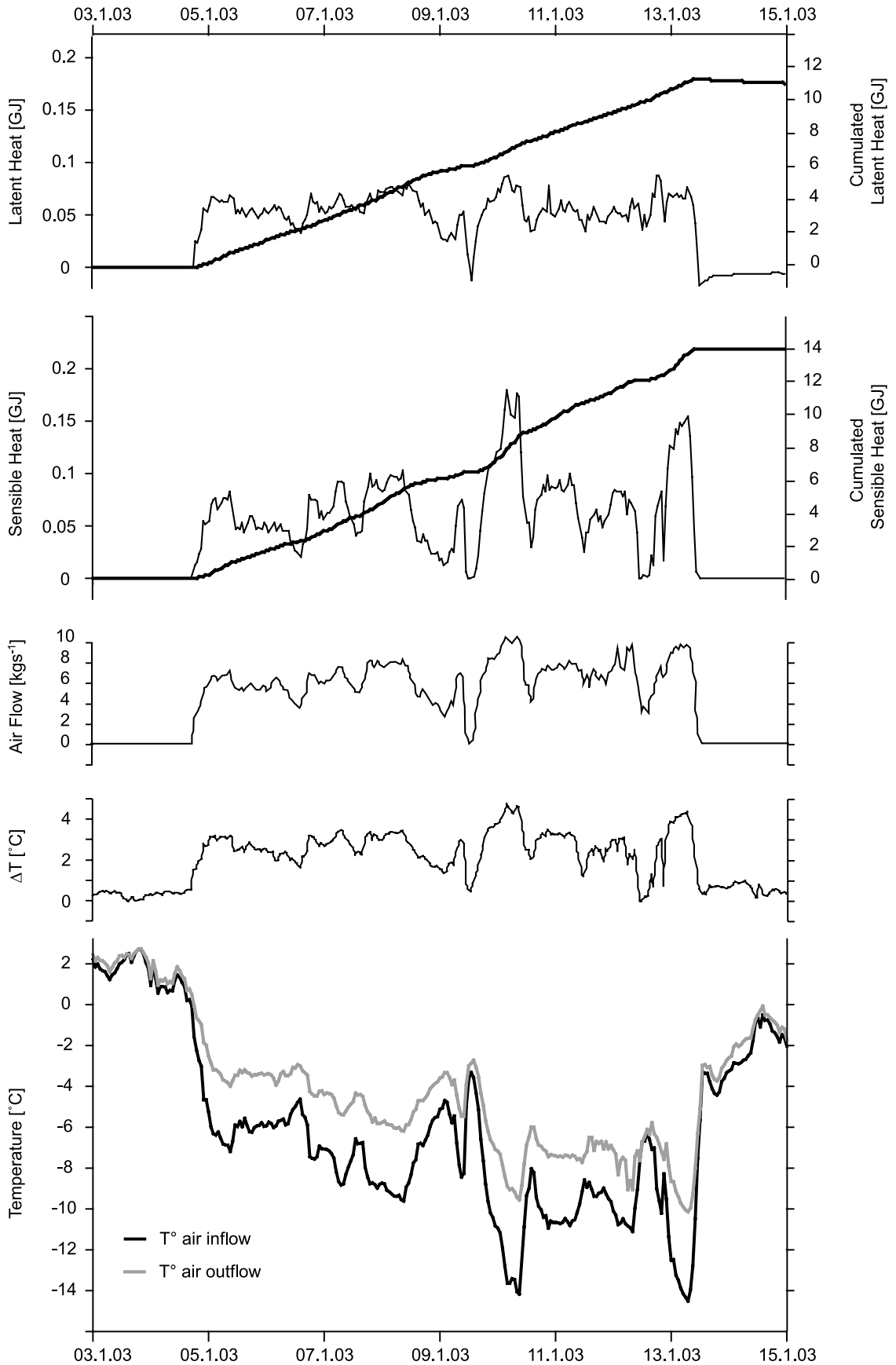
03.1.03
05.1.03
07.1.03
09.1.03
11.1.03
13.1.03
15.1.03
Latent Heat [GJ]
Cumulated Latent Heat [GJ]
Sensible Heat [GJ]
Cumulated Sensible Heat [GJ]
Air Flow [kgs-1]
ΔT [°C]
Temperature [°C]
T° air inflow
T° air outflow

Figure 5

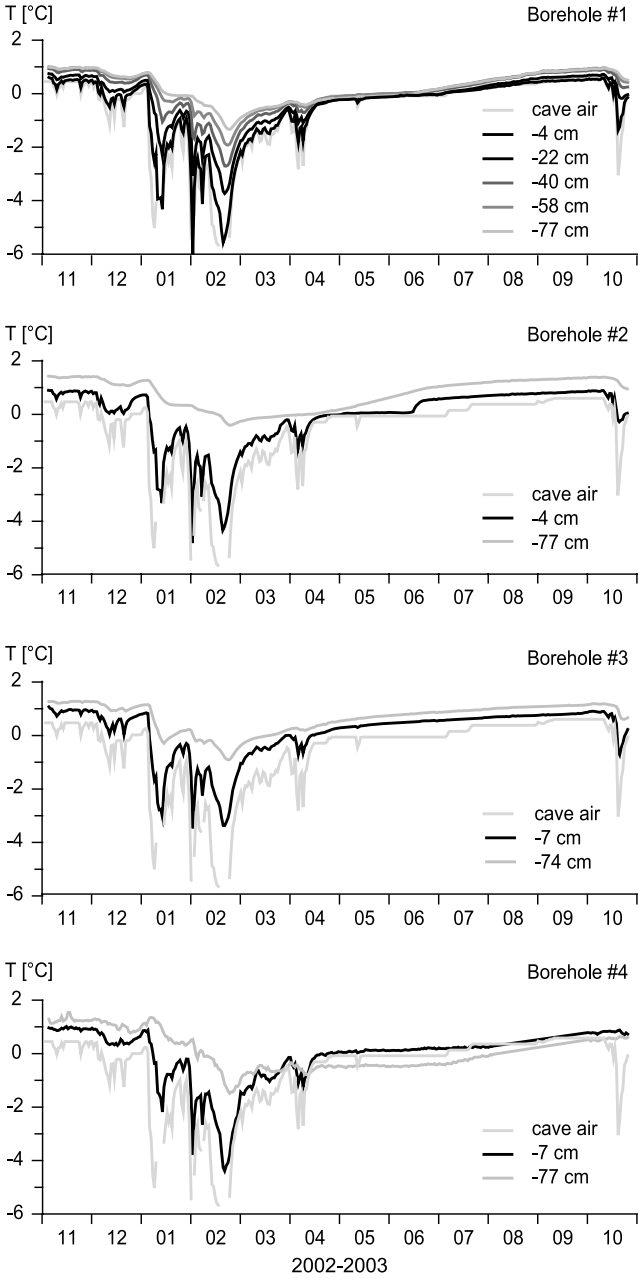

Figure 6. Rock temperatures at different depths measured in four boreholes of Monlesi ice cave between November 2002 and October 2003.

after the first significant rainfall, while the recession ends within 2 d after the peak discharge (mean recession time: ~39 h). This very rapid response and recession suggests a highly transmissive system with a strong direct control from exterior rainfall. Water temperatures show a consistent response with the measured discharge: the maximum water temperature occurs at or immediately after peak flows and approaches 4.5°C, the assumed rock temperature at the system boundaries (equal to the outside mean annual air temperature). However, for lower flows, the heat transfer with the cold rock in the vicinity of the cave is important, and during recessions, water temperatures fall toward 0°C.

[36] Assuming that all the heat advected by water inflow is transferred to the system (i.e., out-flowing water temperature is 0°C for all events), then

$$\Delta E_{\text{water}} = c_w \int_{1\text{year}} Q_m T dt, \tag{12}$$

where ΔE_{water} is energy advected by in-flowing water (J), c_w is heat capacity of water (4180 J kg^{-1} K^{-1}), Q_m is water flow mass rate (kg s^{-1}), and T is water temperature (K).

[37] From equation (12), the thermal contribution of the main water inlet measured during the 2002–2003 annual cycle of 2.2 ± 0.3 GJ. Since our measurements suggest that this inlet drains about half of the water circulating through the cave, the total heat transferred to the cave by water infiltrations is assessed at 4.4 ± 0.6 GJ during the 2002–2003 observation period.

4.5. Heat Advected by Snow Intrusions

[38] Daily measurements of precipitation at the Brevine and Ponts-de-Martel pluviometric stations suggest that Monlesi study site experienced a cumulated snowfall of nearly 2 m during the winter 2002–2003 (i.e., 227 ± 5 mm water equivalent, ρ_{snow} = 100 ± 20 kg m^{-3}). Assuming that snow only enters the ice cave via direct precipitation over the area of the cave entrances (140 ± 5 m^2) and neglecting its sensible heat, then the heat advected by snow intrusions is assessed at −10.6 ± 0.6 GJ (latent heat of snow is 3.35 × 10^5 J kg^{-1}).

4.6. Solar Radiation

[39] Because of the morphology of the cave and the surrounding topography, direct beam solar radiation is almost never observed at the base of the cave entrances. The dense forest canopy at the entrances attenuates the radiation flux, and the high albedo of the snow accumulated at the base of the entrance limits the proportion of the radiation absorbed. It is therefore assumed that heating by direct insolation is negligible, and the contribution of solar radiation to the energy balance is set at 0 GJ.

4.7. Sensible Heat Stored in the Cave Ice

[40] Ice temperatures recorded from November 2002 to August 2003 reveal seasonal temperature oscillations throughout the entire ice volume with a buffering of the signal and a phase shift with depth (Figure 8). Temperatures

Table 1. Heat Fluxes Based on Temperature Measurements in Four 80 cm Long Boreholes Drilled in the Monlesi Cave Walls

Borehole	Observation Period	Δx, m	ΔT, °C	Gradient, °C m^{-1}	Heat Flux, W m^{-2}
1	25 Sep 2003 to 5 Oct 2003	0.73	0.38	0.52	1.1
2	25 Sep 2003 to 5 Oct 2003	0.73	0.51	0.70	1.5
2	1 Aug 2004 to 8 Aug 2004	0.73	0.50	0.68	1.5
3	25 Sep 2003 to 5 Oct 2003	0.67	0.31	0.46	1.0
3	1 Aug 2004 to 8 Aug 2004	0.67	0.32	0.48	1.1
4	4 Nov 2002 to 15 Nov 2002	0.7	0.31	0.44	1.0

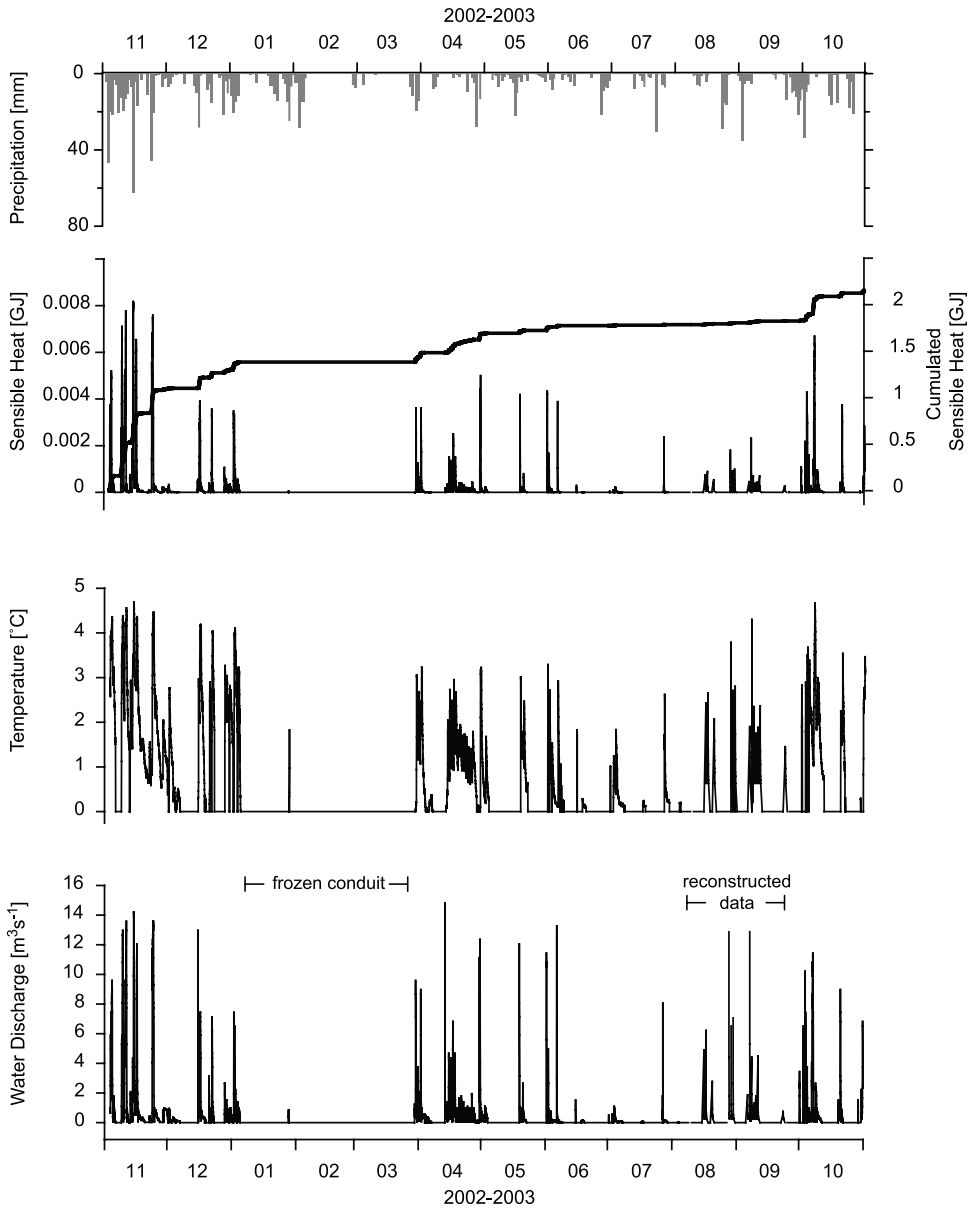

Figure 7. Precipitation, water discharge, and water temperature recorded at the main inlet of Monlesi ice cave during the 2002–2003 observation period. Sensible heat contribution was determined assuming an out-flowing water temperature at 0°C.

measured at −8 m display values close to 0°C, suggesting a temperate ice body subject to (basal) melting at the rock-ice interface. Since the recorded cave ice temperature data reach a thermal equilibrium in mid-August, sensible heat exchanges are not relevant for the annual energy balance of the investigated system, although the winter energy deficit may largely be transferred into summer accumulation of cave ice.

4.8. Fluctuation of Cave Ice Volume

[41] The cave ice volume oscillates with an annual cycle peaking at the start of summer (June–July) and shows minimal values in early winter (December–January) (Figure 9). Measurements of the cave ice surface elevation between June 2001 and March 2007 reveal seasonal variations in the accretion rate of cave ice, with values ranging between 10 and 30 cm a^{-1} (average is 19 ± 8 cm, n = 5). In contrast, annual ablation rates are fairly constant, with a mean annual value of 21 ± 1 cm. When the total ablation exceeds accumulation, an overall negative mass balance occurs. The latter was the case for the 2002–2003 observation period, when the cave ice surface (900 m^2 ± 10%) decreased by nearly 10 ± 0.5 cm. Assuming this value is valid for the entire ice body, the volume of the cave ice lost is assessed at 90 ± 14 m^3. From the latent heat of ice (L_{ice} = 3.35 × 10^5 J kg^{-1}) and a density of 920 ± 20 kg m^{-3}, an energy supply of 28 ± 5 GJ is obtained.

5. Discussion

5.1. Energy Balance

[42] The quantification of heat fluxes at the boundaries of Monlesi cave system identified successfully the order of

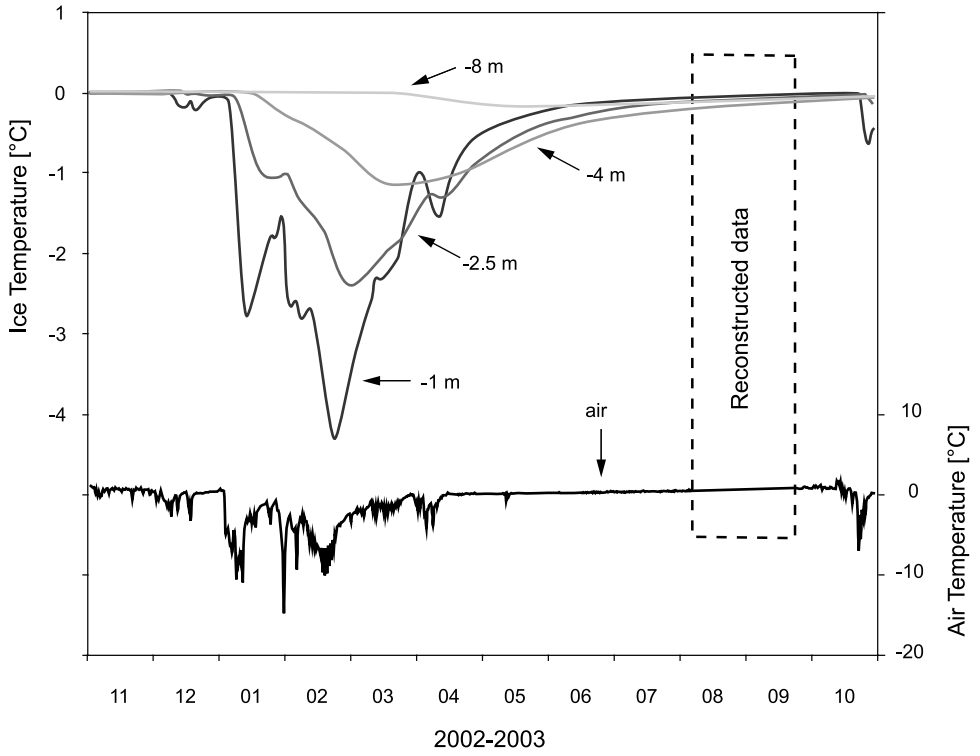

Figure 8. Daily mean temperature recorded at different depths in the ice filling of Monlesi cave.

magnitudes of the individual components involved in the energy balance. The energy balance as given in equation (1) closes within the range of uncertainties, with

$$\begin{aligned}\Delta E_{\text{air}} + E_{\text{rock}} + \Delta E_{\text{water}} + \text{LE}_{\text{snow}} + R \\ = \Delta\text{SE}_{\text{ice}} + \Delta\text{LE}_{\text{ice}}(-75 \pm 8) + (126 \pm 25) + (4.4 \pm 0.6) \\ + (-10.6 \pm 0.6) + (0) = (0) + (28 \pm 5), \qquad (13)\end{aligned}$$

with ΔE_{air} being heat advected by air circulation, E_{rock} being ground heat flux, ΔE_{water} being heat advected by water circulation, LE_{snow} being latent heat of intrusive snow, R being solar radiation, $\Delta\text{SE}_{\text{ice}}$ being sensible heat stored in the cave ice, and $\Delta\text{LE}_{\text{ice}}$ being latent heat of ice (all units given in GJ).

[43] These results suggest that the quantified order of magnitudes are plausible, although major uncertainties remain on some of the individual components. Air circulation due to forced convection during the winter season is shown to be an efficient way to exchange heat between the cave system and the external environment. In order to uncouple the thermal aspect from the problem of motion, it was assumed that the forcing was solely controlled by the temperature difference between the exterior and the subsurface. Although this simplification appears to be reasonable, humidity measurements have shown that significant fluctuations are to be expected during the open period (between November and April). By assuming that out-flowing air was saturated in humidity, latent heat exchanges associated with sublimation of the ice body are thus probably slightly overestimated as compared to sensible heat transfer. Nonetheless, our results confirm earlier observations suggesting that the cave ice mass balance is mostly controlled by winter temperature and precipitation regimes and that summer climatic conditions play a limited effect on the annual mass balance of cave ice [e.g., *Ohata et al.*, 1994; *Luetscher et al.*, 2005]. This is particularly highlighted in Figure 9, where the high temperature observed during the summer 2003 heat wave [e.g., *Beniston*, 2004] seems not to have affected the Monlesi cave ice mass balance. Although this

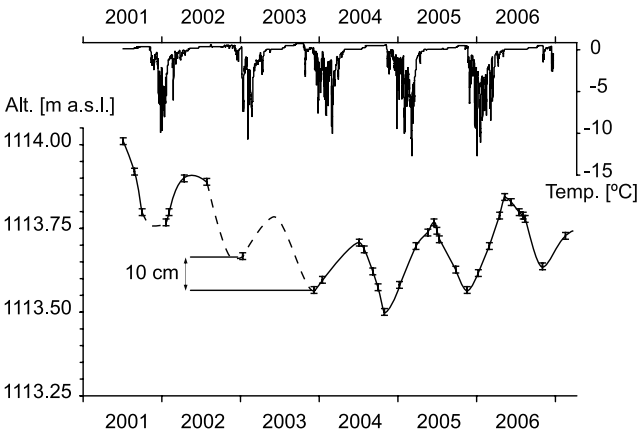

Figure 9. Cave air temperature and ice surface evolution measured in Monlesi ice cave between 2001 and 2007. Manual measurements of the cave ice extension are given with their error bar (±0.5 cm). Cave ice fluctuations are interpolated linearly between available data (smooth black line). In absence of measurements, the seasonal cycles are extrapolated from qualitative field observations (dashed line). The thickness of the cave ice decreased by nearly 10 cm during the 2002–2003 annual cycle.

conclusion further supports the fact that solar radiation can be neglected in the energy balance of the ice cave, long-term changes in the radiation budget will modify the boundary condition of the system and thus also impact on the energy balance of the ice cave. So far, the rapidity of this response is, however, difficult to assess.

[44] Our measurements indicate that the melting of cave ice is mostly controlled by heat exchanges with the host rock. Assuming that boundary conditions within the limestone are defined by a constant temperature, it can be inferred that because of the high thermal inertia of the rock, the melting rate remains almost constant on a decadal timescale. This interpretation is validated by field measurements of the cave ice volume between 2001 and 2007, which show a fairly constant ablation rate of 21 ± 1 cm a^{-1} (Figure 9). However, because the measured ground heat flux of 1 W m^{-2} is about 55% higher than expected by pure heat diffusion through the host rock, advective heat fluxes due to water and air circulation must be present close to the cave walls. This is particularly well illustrated by the higher heat flux measured in borehole 2, which is located along a major fracture feeding the main water inlet. Similarly, a large ''rimaye'' observed on the western side of the cave is attributed to higher heat transfers at the cave walls. Despite the high uncertainties attributed to the accuracy of absolute temperature measurements (i.e., ±0.1°C), the measured heat flux is consistent with an annual melting rate of 8 ± 2 cm a^{-1} measured at the base of the ice volume [*Luetscher et al.*, 2007].

[45] Heat advected by seepage water was estimated from the largest inlet and extrapolated to the entire cave on the basis of manual gauging of individual drip points. However, because the reaction time and thermal response to recharge events is specific to each water inlet, the net contribution to the energy balance could be slightly overestimated. Furthermore, since water temperature at the lower boundary condition was assumed to be at 0°C, the quantified heat contribution has to be considered as a maximal value. It is therefore concluded that seepage water accounts for less than 5% of the total heat supplied to the Monlesi cave system. In contrast, intrusive snow accumulation plays a more significant role in the energy balance of Monlesi ice cave. Heat transfers being most efficient in the presence of seepage water during snowmelt, a reduced snow cover also dramatically limits the formation of new cave ice. This conclusion is again supported by Figure 9, where the decreasing trend observed in the Monlesi cave ice volume between 2001 and 2004 is consistent with external winter climate conditions measured during the same period [*Luetscher et al.*, 2005]. In contrast, the lower external air temperatures and increased snowfall measured during the winter 2004–2005 and 2005–2006 led to positive cave ice mass balances (Figure 9).

[46] Besides the uncertainties remaining on each term of the energy balance, limitations of this model lie in its confinement to one single cave. Since several morphological parameters have to be reconsidered for each system (for instance, dimensions of the entrance pits and exchange surface with the cave air), our quantification cannot be easily extrapolated to other ice caves. Nevertheless, the major processes controlling the energy balance of a cave system could be identified, thus providing the local validation for a conceptual model of heat exchanges in the heterothermic zone of ventilated karst systems.

5.2. Evolution of Subsurface Ice Accumulations

[47] The quantified energy balance of Monlesi ice cave underlines the sensitivity of subsurface ice accumulations to the duration and amplitude of winter temperatures below 0°C. In contrast, the characteristic time for summer temperature response is greater, as it is mainly expressed through conductive heat fluxes in the cave walls. Although the contribution of rainfall to the energy balance is limited, the precipitation regime is assumed to play a significant role in the formation of cave ice. It is suggested that the maximum cave ice growth is reached during the daily melting of the snow cover followed by freezing nights. Since the frequency of oscillating freeze/thaw cycles at a given altitude may increase with a warming climate, it is concluded that a positive mass balance can still be observed if external winter temperatures fluctuate around 0°C.

[48] However, on a century timescale, external temperature fluctuations will inexorably modify the boundary conditions in the host rock. Under a warming climate scenario, ground heat fluxes would increase according to the long-term trend of MAAT, and a general increase of subsurface cave ice melting rates is to be expected. This, together with warmer winter temperatures and reduced snow precipitation at low altitude, would lead to the progressive disappearing of perennial ice bodies in numerous low-altitude ice caves in temperate regions.

6. Conclusions

[49] Understanding the relationship between the external climate and the cave environment is a major concern for numerous cave studies, including speleothem-based paleoenvironmental reconstructions [e.g., *Fairchild et al.*, 2006]. For the first time, the energy balance of a cave system, and thus a quantification of its different components, was formulated. Generally, the thermal stability observed in caves is controlled by the host rock which buffers subsurface heat exchanges [e.g., *Badino*, 1995; *Lismonde*, 2002]. However, it could be demonstrated that in specific sections of a cave system, heat transfers due to forced air convection can be dominant, leading to significant thermal anomalies as compared to the mean annual air temperature. Such anomalies can be negative (as, for instance, in ice caves) but also positive, with sections being abnormally warm in the upper entrance zone of a ventilated cave system. Empirical observations from alpine ice caves suggest that this heterothermic zone may extend over several hundreds of meters from the cave entrance, depending on the cave morphology (e.g., Eisriesenwelt, Austria).

[50] Although smaller variations in the external climate do not significantly affect the extension of the heterothermic zone, morphological changes at the cave entrances (e.g., flooding, collapse, and erosion) could modify dramatically the subsurface ventilation regime. These changes will affect not only the temperature distribution in the cave system but also the spatial variability of humidity and CO_2 concentrations. In the author's opinion, understanding the mechanisms controlling the subsurface environment represents a

major prerequisite for high-resolution paleoenvironmental reconstructions from cave deposits.

[51] **Acknowledgments.** The authors would like to acknowledge François Bourret, who provided critical help in the instrumentation of Monlesi ice cave. P. L. Smart made helpful comments and edits on an early version of the manuscript, and thorough reviews of D. Lacelle and C. Smart greatly improved the final version. This work has been supported by the Swiss National Science Foundation, projects 21-63764.00 and PBZH2-112727.

References

Andrieux, C. (1969), Contribution à l'étude du climat des cavités naturelles des massifs karstiques, Ph.D. thesis, 240 pp., Univ. de Bordeaux, Bordeaux, France.

Atkinson, T. C., P. L. Smart, and T. M. L. Wigley (1983), Climate and natural radon levels in Castleguard cave, Columbia Icefields, Alberta, Canada, *Arct. Alp. Res.*, *15*, 487–502, doi:10.2307/1551235.

Badino, G. (1995), *Fisica del Clima Sotterraneo*, *Mem. Ist. Ital. Speleologia Ser. II*, vol. *7*, 136 pp., Istituto Italiano di Speleologia, Bologna, Italy.

Balch, E. S. (1970), *Glacières or Freezing Caverns*, Johnson, New York.

Baldini, J. U. L., L. M. Baldini, F. McDermott, and N. Clipson (2006), Carbon dioxide sources, sinks, and spatial variability in shallow temperate zone caves: Evidence from Ballynamintra Cave, Ireland, *J. Cave Karst Stud.*, *68*(1), 4–11.

Beniston, M. (2004), The 2003 heat wave in Europe: A shape of things to come? An analysis based on Swiss climatological data and model simulations, *Geophys. Res. Lett.*, *31*, L02202, doi:10.1029/2003GL018857.

Bock, H. (1913), Mathematisch-physikalische untersuchung der eishöhlen und windröhren, in *Die Höhlen im Dachstein*, edited by H. Bock, G. Lahner, and G. Gaunersdorfer, Ver. Höhlenkunde Oesterreich, Graz, Austria.

Bourges, F., A. Mangin, and D. D'Hulst (2001), Carbon dioxide in karst cavity atmosphere dynamics: The example of the Aven d'Orgnac (Ardeche), *C. R. Acad. Sci., Ser. IIA: Terre Planetes*, *333*(11), 685–692.

Bourges, F., P. Genthon, A. Mangin, and D. D'Hulst (2006), Microclimates of l'Aven d'Orgnac and other French limestone caves (Chauvet, Esparros, Marsoulas), *Int. J. Climatol.*, *26*, 1651–1670, doi:1002/joc.1327.

de Freitas, C. R., and R. N. Littlejohn (1987), Cave climate: Assessment of heat and moisture exchange, *Int. J. Climatol.*, *7*, 553–569, doi:10.1002/joc.3370070604.

de Freitas, C. R., and A. Schmekal (2003), Condensation as a microclimate process: Measurement, numerical simulation and prediction in the Glowworm Cave, New Zealand, *Int. J. Climatol.*, *23*, 557–575, doi: 10.1002/joc.898.

de Freitas, C. R., R. N. Littlejohn, T. S. Clarkson, and I. S. Kristament (1982), Cave climate: Assessment of airflow and ventilation, *J. Climatol.*, *2*, 383–397, doi:10.1002/joc.3370020408.

Dueñas, C., M. C. Fernandez, S. Canete, J. Carretero, and E. Liger (1999), Rn-222 concentrations, natural flow rate and the radiation exposure levels in the Nerja Cave, *Atmos. Environ.*, *33*(3), 501–510.

Fairchild, I. J., C. L. Smith, A. Baker, L. Fuller, C. Spötl, D. Mattey, and F. McDermott (2006), Modification and preservation of environmental signals in speleothems, *Earth Sci. Rev.*, *75*(1–4), 105–153.

Hendy, C. H. (1971), The isotopic geochemistry of speleothems—I. The calculation of the effects of different modes of formation on the isotopic composition of speleothems and their applicability as paleoclimatic indicators, *Geochim. Cosmochim. Acta*, *35*, 801–824, doi:10.1016/0016-7037(71)90127-X.

Incropera, F. P., and D. P. DeWitt (2002), *Fundamentals of Heat and Mass Transfer*, 5th ed., 981 pp., John Wiley, New York.

Johnson, K. R., C. Y. Hu, N. S. Belshaw, and G. M. Henderson (2006), Seasonal trace-element and stable-isotope variations in a Chinese speleothem: The potential for high-resolution paleomonsoon reconstruction, *Earth Planet. Sci. Lett.*, *244*(1–2), 394–407.

Lacelle, D., B. Lauriol, and I. D. Clark (2004), Seasonal isotopic imprint in moonmilk from Caverne de l'Ours (Quebec, Canada): Implications for climatic reconstruction, *Can. J. Earth Sci.*, *41*(12), 1411–1423, doi:10.1139/e04-080.

Lismonde, B. (2002), Aérologie des systèmes karstiques, report, 362 pp., Com. Dép. de Spéléologie Isère, Grenoble, France.

Luetscher, M. (2005), Processes in ice caves and their significance for paleoenvironmental reconstructions, Ph.D. thesis, Univ. of Zurich, Zurich, Switzerland.

Luetscher, M., and P.-Y. Jeannin (2004a), Temperature distribution in karst systems: The role of air and water fluxes, *Terra Nova*, *16*, 344–350, doi:10.1111/j.1365-3121.2004.00572.x.

Luetscher, M., and P.-Y. Jeannin (2004b), The role of winter air circulations for the presence of subsurface ice accumulations: An example from Monlesi ice cave, *Theor. Appl. Karstology*, *17*, 19–25.

Luetscher, M., P.-Y. Jeannin, and W. Haeberli (2005), Ice caves as an indicator of winter climate evolution: A case study from the Jura Mountains, *Holocene*, *15*, 982–993, doi:10.1191/0959683605h1872ra.

Luetscher, M., D. Bolius, M. Schwikowski, U. Schotterer, and P. L. Smart (2007), Comparison of techniques for dating of subsurface ice from Monlesi ice cave, Switzerland, *J. Glaciol.*, *53*(182), 374–384, doi:10.3189/002214307783258503.

McDermott, F. (2004), Palaeo-climate reconstruction from stable isotope variations in speleothems: A review, *Quat. Sci. Rev.*, *23*, 901–918, doi:10.1016/j.quascirev.2003.06.021.

Ohata, T., T. Furukawa, and K. Osada (1994), Glacioclimatological study of perennial ice in the Fuji Ice cave, Japan. 2. Interannual variation and relation to climate, *Arct. Alp. Res.*, *26*, 238–244, doi:10.2307/1551936.

Piasecki, J., T. Sawinski, K. Strug, and J. Zelinka (2006), Selected characteristics of the microclimate of the Demanovska Ice Cave (Slovakia), paper presented at the 2nd International Workshop on Ice Caves IWICII, Demanovska Dolina, Slovak Republic, May 8–12.

Roberts, M. S., P. L. Smart, and A. Baker (1998), Annual trace element variations in a Holocene speleothem, *Earth Planet. Sci. Lett.*, *154*(1–4), 237–246, doi:10.1016/S0012-821X(97)00116-7.

Saar, R. (1956), Eishoehlen, ein meteorologisch-geophysikalisches Phanomen. Untersuchungen and der Rieseneishoehle (R.E.H.) im Dachstein, Oberösterreich, *Geogr. Ann.*, *38*(1), 1–63, doi:10.2307/520404.

Spötl, C., I. J. Fairchild, and A. F. Tooth (2005), Cave air control on dripwater geochemistry, Obir Caves (Austria): Implications for speleothem deposition in dynamically ventilated caves, *Geochim. Cosmochim. Acta*, *69*, 2451–2468, doi:10.1016/j.gca.2004.12.009.

Wigley, T. M. L., and M. C. Brown (1971), Geophysical applications of heat and mass transfer in turbulent pipe flow, *Boundary Layer Meteorol.*, *1*, 300–320, doi:10.1007/BF02186034.

Wigley, T. M. L., and M. C. Brown (1976), Cave meteorology, in *The Physics of Caves*, edited by T. D. Ford and C. H. D. Cullingford, Elsevier, New York.

P.-Y. Jeannin, Swiss Institute for Speleology and Karstology, P.O. Box 818, CH-2301 La Chaux-de-Fonds, Switzerland.

B. Lismonde, Laboratory of Geophysical and Industrial Fluid Flows, Domaine Universitaire, BP 53, F-38041 Grenoble, CEDEX 9, France.

M. Luetscher, Institute of Geology and Paleontology, University of Innsbruck, A-6020 Innsbruck, Austria. (marc.luetscher@uibkl.ac.at)